Flexible Automatic Generation Control System for Embedded HVDC Links

Francisco Gonzalez-Longatt
Loughborough University
School of Electric, Electronic and Systems Engineering
Loughborough, United Kingdom
fglongatt@fglongatt.org

Anton Steliuk
DMCC Engineering Ltd
Peremogy ave., 56, Kyiv, 03056
Ukraine
anton.stelyuk@dmcc.com.ua

Víctor Hugo Hinojosa M
Universidad Técnica Federico Santa María, Department of Electrical Engineering Valparaiso-Chile
victor.hinojosa@usm.cl

***Abstract*— Future power systems are expected being operated under increasingly stressed conditions and increased uncertainties. The future single European electricity market will entail higher energy trading volumes, for which augmented use of HVDCs is expected to facilitate cross-border bulk power transfers. In traditional power systems a change in demand at one point of network is reflected throughout the system by a change in frequency. However, significant interconnections using HVDC will affect the classical ability of traditional AC system to overcome "together" frequency deviations which may result in a cascading failure and system collapse. Future HVDC systems shall fulfil requirements referring to frequency stability and also intervening in the frequency quality. As consequence HVDC systems will operate providing ancillary service depends on the framework of service. This paper proposes a flexible *Automatic Generation Control* (AGC) system for embedded HVDC links in order to provide frequency sensitive response and control power interchange.**

***Index Terms*-- Automatic generation control, frequency controller, frequency stability, power system, protection scheme, wind turbine generator.**

I. Introduction

Future energy systems networks will be completely different to the power systems on nowadays [1], [2]. High and low power converters will be massively deployed in several areas on the electric network [3], [4]: (i) renewable energy from highly variable generators connected over high power converters, (ii) several technologies for energy storage with very different time constants, some of them using power converters as an interface to the grid, and (iii) Pan-European transmission network facilitating the massive integration of large-scale renewable energy sources and transportation of electricity based on underwater *multi-terminal high voltage direct current* transmission. The developments of stronger interconnector and massive integration of offshore wind power in remote location are steadily increasing the demand for more robust, efficient, and reliable grid integration solutions. Multi-terminal *Voltage source converter* (VSC)-based HVDC (MTDC) technology has the potential to increase transmission capacity, system reliability, and electricity market opportunities.

The integration of VSC-HVDC links into transmission systems has the potential to afford a powerful new tool for controlling both over and under frequency conditions. The high degree of controllability inherent to the active power flow on HVDC links allow rapid changes of power flows to be used to counter active power imbalances [5].

Primary frequency control in HVDC has been a hot topic in recent times. Several publications have developed and tested controllers to enable *inertial response* on HVDC systems [6-9]. HVDC for primary frequency control has been considered in several publications [10], [11], and the coordinated primary frequency control among non-synchronous systems connected by a multi-terminal HVDC grid has been studied in [12]. In addition, the problem of providing frequency control services, including inertia emulation and primary frequency control, from offshore wind farms connected through a MTDC network has been studied in [13]. However, *secondary* and *tertiary frequency control* considering HVDC or MTDC systems has deserved a very low attention in recent publications.

This paper proposes a flexible *Automatic Generation Control* (AGC) system for embedded HVDC link in order to provide frequency sensitive response and control power interchange. The paper is organized as follows: Section II briefly defines the main considerations about *DC-Independent System Operator* (DC-ISO) and Section III establishes the short backgrounds about DC-voltage control in MTDC systems. Section IV focuses the proposed optimal power flow in system based on DC-ISO objectives. Section V illustrates application examples on a representative test system of a future DC-ISO. Finally, section VI results are tabulated for assessment and comparisons.

II. FREQUENCY CONTROL

Frequency control in power systems is usually formed of *primary* and *secondary control*. Future power system will require an active participation of HVDC to support the primary and secondary frequency control.

Frequency control can be considered to be one of the most crucial aspects of ancillary services. It is responsible that the power system operates within acceptable frequency limits. The classical approach of frequency control can schematically be divided by three stages: *primary*, *secondary* and *tertiary control*. This is a tiered approach where controllers are responsible of frequency containment, frequency restoration and replacement reserves, respectively.

The primary control refers to control actions that are done locally (on the power plant level) based on the set-points for frequency and power. The objective of the primary control is to maintain the balance between generation and load [1] as consequence stabilizes the frequency after a disturbance. The primary frequency controllers are typically a simple proportional controller. A generating unit participating in primary control uses a proportional constant in the controller, named *speed droop D*. The constant provides the relationship between momentary frequency deviation (Δf) and change in electric power production (ΔP), $D = \Delta f / \Delta P$ in Hz/MW

Post-disturbance steady-state frequency differs from the nominal frequency, especially because the droop characteristics in primary controllers and the load self-regulation effect. The secondary frequency control, also called *Load Frequency Control* (LFC), adjusts power set-points of the generators in order to compensate for the remaining frequency error after the primary control has acted.

The purpose of secondary control actions is to restore the system frequency to the nominal set point, and ensure that any tie-line flows in the system are at their contracted level. LFC can also be performed manually as in case of the Nordel powers system and [14], Continental Europe interconnected system (ENTSO-e) and *National Grid Transco* (NGT) in England and Wales [15], uses an automatic scheme which can also be called *Automatic Generation Control* (AGC). Global analysis of the power system markets shows that the AGC is one of the most profitable ancillary services at these systems [16].

The AGC is a controller created for the following functions [17]: (i) maintain frequency at the scheduled value (frequency control); (ii) maintain the net power interchanges with neighboring control areas at their scheduled values (tie-line control); and (iii) maintain power allocation among the units in accordance with area dispatching needs (energy market, security or emergency).

In some interconnected power systems, the role of AGC may be restricted one or two of the above objectives. For instance, tie-line power control is only used where a number of separate power systems are interconnected and operate under mutually beneficial contractual agreements.

Based on the above objectives, two variables frequency and tie line power exchanges are weighted together and used into the supplementary feedback loop. A suitable linear combination of frequency ($\Delta f_i = f_i - f_{set}$) and tie-line power changes ($\Delta P_{tie,i} = P_{tie,i} - P_{tie,i}^{set}$) for area i, is known as the *Area Control Error* (ACE):

$$ACE_i = -\Delta P_{tie,i} + \beta_{bias,i} \Delta f_i \quad (1)$$

where $\beta_{bias,i}$ is a bias factor. *ACE* corresponds to the power by which the total area power generation must be changed in order to maintain both frequency and tie-line flows at their scheduled values. The AGC is a central frequency regulator which uses an integrating element in order to remove any error and this may be supplemented by a proportional element. For such a PI regulator the output signal is:

$$P_{AGC,i} = K_{P,i} ACE_i + K_{I,i} \int ACE_i dt \quad (2)$$

The aim of the frequency bias factor $\beta_{bias,i}$ is to fully compensate for the initial frequency response of the area. It can be demonstrated that independent of the choice of $\beta_{bias,i}$ the frequency deviation will eventually be returned to zero so that the choice of $\beta_{bias,i}$ is not critical for the system. The regulator in an area tries to restore the frequency and net tie-line interchanges after an imbalance, so it enforces an increase in generation equal to the power deficit. The regulation is executed by changing the power output of power plants in the area through varying $P_{ref,i}$ in their governing systems.

The regulator output signal ΔP_{ref} is then multiplied by the participation factors α_1, α_2, …, α_n which define the *contribution of the individual generating units* to the total generation control as shown on Fig 1.

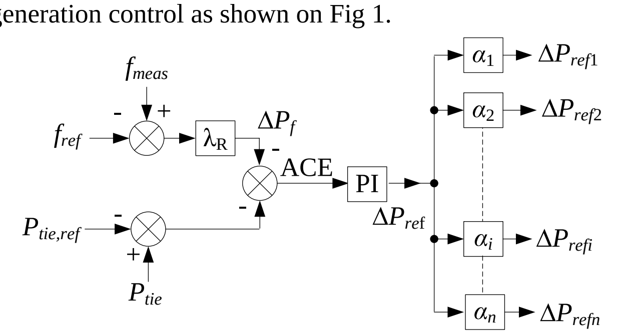

Figure 1. Functional diagram of a central regulator [17].

The control signals ΔP_{ref1}, ΔP_{ref2}, …, ΔP_{refn} obtained in this way are then transmitted to the power plants and delivered to the reference set points of the turbine governing systems. During the last decades, there has been a large amount of research into alternatives to the classical AGC control formulation. With the advent of advanced control theory many new solutions have been proposed. A summary of the research into such topics is provided in [18], [19].

III. AUTOMATIC GENERATION CONTROL (AGC)

The structure of the AGC of the *interconnected power system* (IPS) is shown in Fig. 2. It consists of n power plants with generation units participating in frequency support.

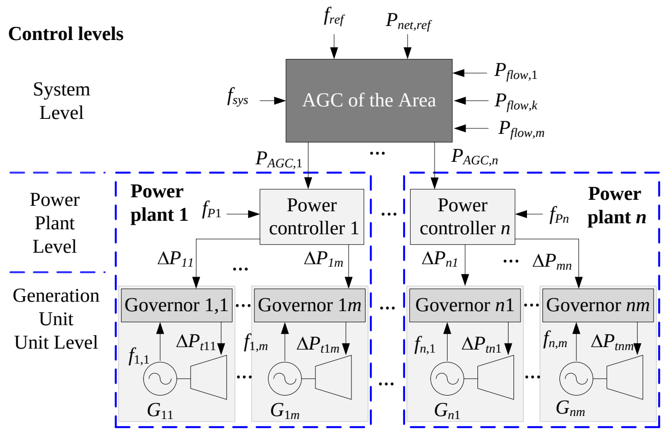

Figure 2. The structure of the Interconnected Power system and representation of the AGC.

There are three control levels of the active power and frequency control. The upper system control level is presented by the AGC of the area (*system level*). The input signals are the system frequency measurement $f_{meas}=f_{sys}$ in the power system, and the scheduled power on the interface (P_{tie} line interchanges $P_{flow,k}$.

Based on *tie-line interchanges* $P_{flow,k}$, the net *interchange power* ($P_{net,ref}$) is calculated by:

$$P_{net,ref} = \sum_{k=1}^{N_{branches}} P_{flow,k} \tag{3}$$

In the AGC of the IPS, the system frequency deviation (Δf) and the changes on the net interchange power (ΔP_{net}) deviations are defined as:

$$\Delta f = f_{sys} - f_{ref} \tag{4}$$

$$\Delta P_{net} = P_{net} - P_{net,ref} \tag{5}$$

where: f_{ref} is a frequency set point value (typically, the rated or nominal frequency), $P_{net.ref}$ is a net interchange power set point value.

The *area control error* (ACE) is calculated in similar way to (1) as:

$$ACE = -\Delta P_{net} + K_{bias}\Delta f \tag{6}$$

where: K_{bias} is the *frequency bias*.

In the event of *internal* power imbalance of the IPS, *ACE* defines the power to be compensated by the regulating power plants in this IPS [20]. In case of *external* frequency disturbance, due to different signs of frequency and net interchange power deviations, ACE value tends to zero. The AGC operation depends on location of the disturbance [20], [21].

The unscheduled active power setting P_{AGC} formed by the *proportional-integral* (PI) controller is calculated as follows:

$$P_{AGC} = K_P ACE + K_I \int_{t_1}^{t_2} ACE dt \tag{7}$$

where: K_P is the proportional gain of the PI controller; K_I is the integral gain of the PI controller; t_1, t_2 are the integration limits. As shown in Fig. 2, the *i*-AGC control signal P_{AGCi}, is transmitted to each regulating power plant according to *the participation factor* α_i of each individual power plant in the secondary frequency control:

$$P_{AGC,i} = \alpha_i P_{AGC} \qquad i = 1, 2, \ldots, n \tag{8}$$

At the *power plant control level* the signal P_{PCi} formed by the power plant PI controller is calculated as:

$$P_{PCi} = K_P^{PC}\left(K_f \Delta f + \Delta P_{agci} - \sum_{j=1}^{m}\Delta P_{Tj}\right) + K_I^{PC}\int_{t_1}^{t_2}\left(K_f \Delta f + \Delta P_{agci} - \sum_{j=1}^{m}\Delta P_{Tj}\right)dt \tag{9}$$

where: K_P^{PC} is the proportional gain of the power plant PI controller; K_I^{PC} is the integral gain of the power plant PI controller; K_f is the coefficient of frequency correction; $\Sigma\Delta P_T$ is the sum of the turbine power change of the generating units participating in the secondary frequency control, and i = 1, 2, …, n,.

The distribution of the control signal P_{PCi} at the *i*-power plant control level is performed in accordance with the participation factors β_{ij} of the generating units in the secondary frequency control (see Fig. 2):

$$\Delta P_{ij} = \beta_{ij} P_{PCi} \quad i = 1, 2, \ldots, n \text{ and } j = 1, 2, \ldots, m \tag{10}$$

where: n is the number of regulating power plants; m is the number of generating units of the *i*-power plant; ΔP_{ij} is the control signal from the power plant controller. The control signal $\Delta P_{ij.ref}$ is distributed in such a way that:

$$P_{PCi} = \sum_{j=1}^{m} \Delta P_{ij} \qquad i = 1, 2, \ldots, n \tag{11}$$

and

$$P_{agc} = \sum_{i=1}^{n} P_{agci} = \sum_{i=1}^{n}\sum_{j=1}^{m} \Delta P_{ij} \tag{12}$$

The calculated control signal ΔP_{ij} from the power controller is transmitted to the turbine governor of the generating unit (*aggregate control level*) using the speed changer motor (see Fig. 2). Further, according to the reference control signal ΔP_{ij}, the turbine governor generates a signal for the turbine power change ΔP_{tij}. Thus, the power changing of the generating units restores the normal frequency and scheduled net interchange power.

IV. Proposed AGC including Embedded HVDC Link

Future power system will require an active participation of HVDC grids to support the AGC function of frequency control. The classical approach presented on Section III is expanded to a hybrid AC/DC system where a HVDC link is embedded in a traditional AC system. The structure of the proposed controller enabling the participation of HVDC link on the AGC support is presented in Fig. 3. There are four control levels of the active power and frequency control. The upper system control level is presented by the AGC of the power system. The input signals are the system frequency measurement f_{meas} in the power, the scheduled power on the interface (P_{tie}) and line interchanges (AC lines: $P_{flow,k}$, and DC lines: $P_{DC,ij}$).

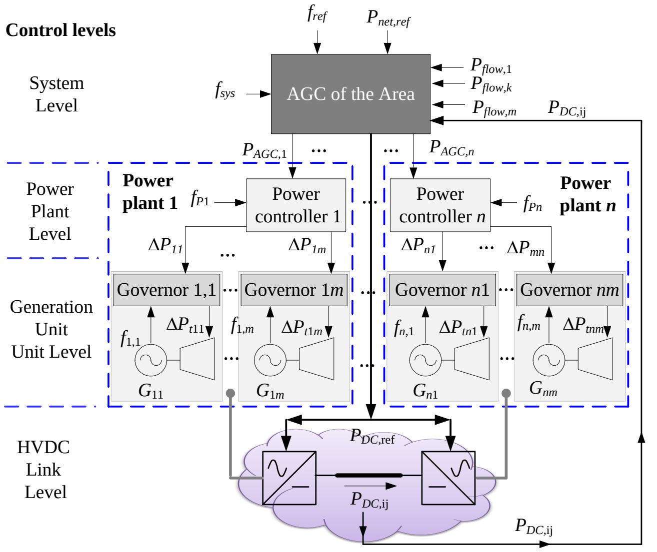

Figure 3. The structure of the hybrid AC/DC Interconnected Power system and considering the proposed AGC controller.

Based on *tie-line interchanges*, the net *interchange power* ($P_{net,ref}$) is calculated as:

$$P_{net,ref} = \sum_{k=1}^{N_{branches}} P_{flow,k} + P_{DC,ij} \tag{13}$$

In the AGC of the power system, the system *frequency deviation* (Δf) and changes on the net interchange power (ΔP_{net}) deviations are calculated using (4) and (5). Also the ACE is calculated using (6). In this paper, the proposed AGC includes a control system to provide signals to embedded HVDC links in order to provide frequency sensitive response and control power interchange. The control is designed to make use of the fast response and lower loses of the HVDC system and alleviate the AC transmission system in the interface between the ISPs. A proportional controller is used to define the change on the HVDC based on the AGC:

$$P_{DC,ref} = P^0_{DC,ref} + \gamma_{HVDC} ACE \tag{14}$$

subject to:

$$P^{\min}_{DC} \le P_{DC,ref} \le P^{\max}_{DC} \tag{15}$$

where $P^0_{DC,ref}$ is pre-contingency power flow on the HVDC link and $P^{\max}_{DC}$, $P^{\min}_{DC}$ power limit of the converter station.

V. Simulation and Results

In this Section, a hybrid AC/DC test network is used to illustrate and test the proposed controller. The classical IEEE 14-bus test system is used as AC test network. It represents a portion of the American Electric Power System (in the Midwestern USA) in February, 1962. The original IEEE 14-bus system (as presented on [22], [23]) has been slightly modified, so the system has three Power Plants and a boundary has been defined to establish 2 operational areas (Area 1 and Area 2 in Fig. 4). Not depicted in Fig. 4, but included in the system model, are generator controllers (IEEE Type 1 speed-governing model and the automatic voltage regulators - SEXS, *Simplified Excitation System*).

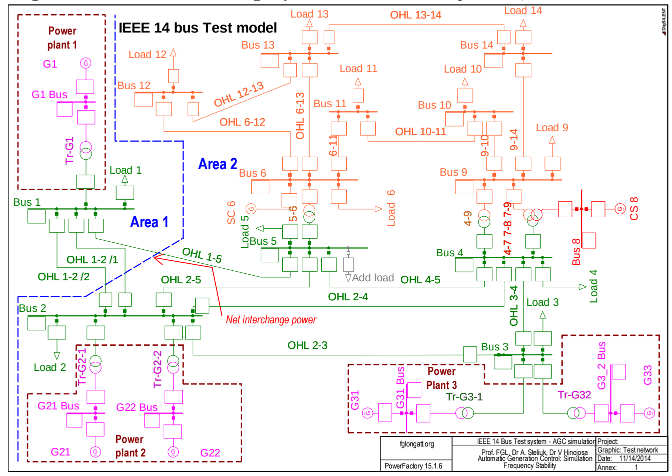

Figure 4: *Test System*: Modified IEEE 14-bus test system.

The interface between Area 1 and Area 2 is defined by three overhead transmission line OHL 1-5, OHL 1-2/1 and OHL 1-2/2, as consequence the AGC is developed to monitor and control the net power interchange on them.

DIgSILENT® PowerFactory™ is used for time-domain (RMS) simulations and *DIgSILENT Simulation Language* (DSL) is used for dynamic modelling of all controllers.

All simulations are performed using a PC based on Intel®, Core™ i7-7410HQ CPU 2.5GHz, 16 GB RAM with Windows 8.1 64-bit operating system.

The proposed AGC model enabling the participation of the HVDC link in the AGC support has been developed using DSL. Figure 5 shows the DSL implementation of the generic AGC controller. Active power flow measurements on OHL 1-5 (P_{flow1}), OHL 1-2/1 (P_{flow2}), and OHL 1-2/2 (P_{flow3}) are used for monitoring the net power interchange. In addition, a measurement device (*ElmPphi*) is used to obtain the system frequency (f_{sys}).

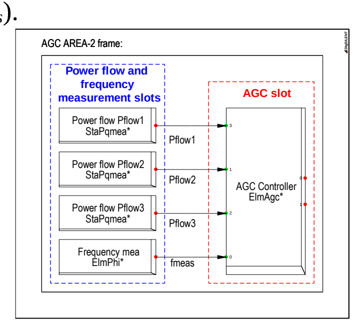

Figure 5. General frame of the AGC model.

Fig. 6 shows the DSL model created for the proposed controller, including the classical AGC and enhancing the participation of the HVDC link in frequency control. Five subsystems have been highlighted on the general frame: Frequency deviation calculation, Calculation of net interchange power deviation, PI controller, signals calculation of the AGC and HVDC contribution.

Three scenarios have been simulated in order to evaluate the performance of the controllers and to demonstrate the suitable operation of the proposed controllers:

– *Case I, No AGC*: This simulation scenario is based on the AC network (IEEE 14-bus) and considering the inertial and governor response. AGC is not active in this case. The idea of this base case is to demonstrate that a system frequency disturbance creates power imbalance which is covered by the governors, however, the final operational frequency is reduced by the action of the droop.
– *Case II: Classic AGC*: A classic AGC controller is enabled in this simulation scenario allowing the frequency recovery after the system frequency disturbance.
– *Case III: Proposed AGC*: under this scenario the HVAC overhead transmission line OHL1-5 is substituted by a HVDC link. Now, the proposed AGC is enabled in the hybrid AC/DC network in order to test the proposed controller.

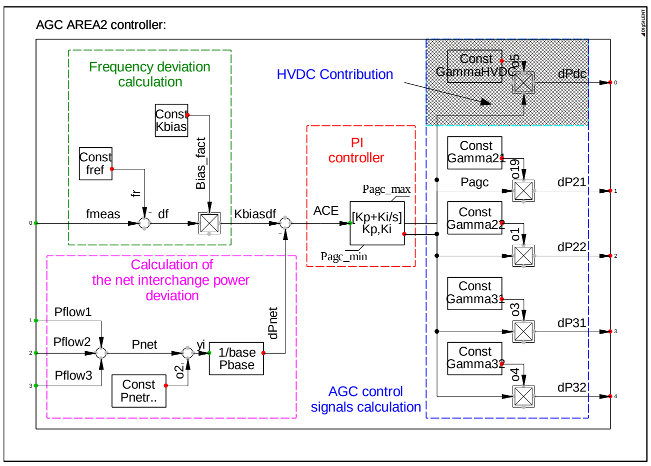

Figure 6. General frame of the Proposed AGC control model.

TABLE I. SUMMARY OF SIMULATION RESULTS

	Case	I	II	III
	Initial state	Post-contingency Steady State		
Output Power at Generators (MW)				
Gen 1	225 (221.3)	232.4	225.3	221.2
Gen 21	150 (148.9)	157.0	160	159.3
Gen 22	150 (148.9)	157.0	160	159.3
Gen 31	150 (148.9)	157.0	159	159.4
Gen 32	150 (148.9)	157.0	159	159.4
Power flows (MW)				
OHL 1-2/1	-17 (-16.2)	-16.4	-13.5	-9.5
OHL 1-2/2	-16.9 (-16.1)	-16.3	-13.5	-9.4
OHL 1-5	-56.3	-64.9	-63.5	--
HVDC	--56.6	–	–	-70.2
Net flow	-90.2 (-88.6)	-97.7	-90.6	-89.1

Number between parentheses shows the initial condition of *Case III*. The use of HVDC link reduces power losses as consequence power generations and power flows are different.

A simple contingency is simulated, it is an events based on step increase on the power demand at load 6 (ΔP_{L6} = 44.8 MW). Plots of main electromechanical associated to the system frequency response are shown on Fig. 6 and 7. *Case II* is used to illustrate how the steady-state post contingency frequency is recovered after the system frequency event, without AGC (*Case I*) a decreased frequency, 49.94 Hz is observed. Also, the positive effect of the classical AGC (*Case II*) on reestablishing the net interchange power flow at the interface is shown on Fig. 7. A summary of the pre and post contingency steady-state, power generation and power flows, for several cases is shown on Table I. Results on Table I demonstrate the capacity of the proposed controller (Case III) to modify the power flow on the interface increasing the power transfer on the HVDC link, decreasing the power on OHL 1-1/2 and OHL 1-2/2 (around -44%), also the correct performance is shown on the faster recovery on the frequency compare to Case II.

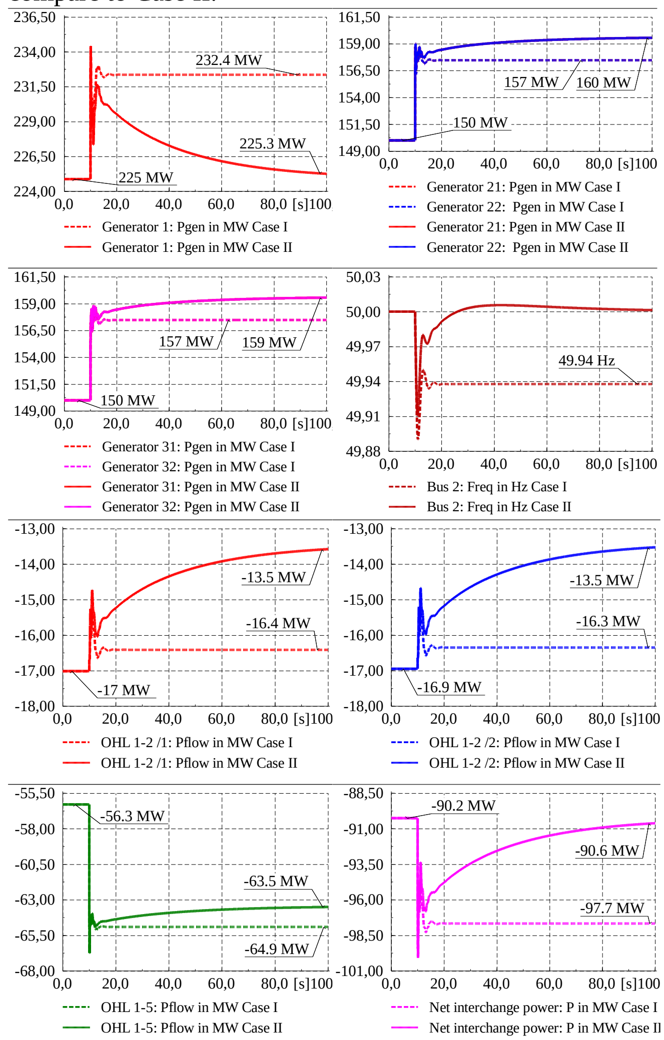

Figure 7. Plots of main electromechanical: *Case I* and *Case II.*

VI. CONCLUSIONS

This paper proposes a flexible AGC system for embedded HVDC link. The proposed AGC includes a control system to provide signals to embedded HVDC links in order to provide frequency sensitive response and control power interchange. The control is designed to make use of the fast response and lower loses of the HVDC system and alleviate the AC transmission system in the interface between the ISPs. A proportional controller is used to define the change on the HVDC based on the AGC and a limiter is included to avoid the overloading the HVDC link. This is a simple an efficient solution to provided frequency support and minimizing the impact on the AC system. Simulations results using a test network demonstrate the correct performance of the proposed controller.

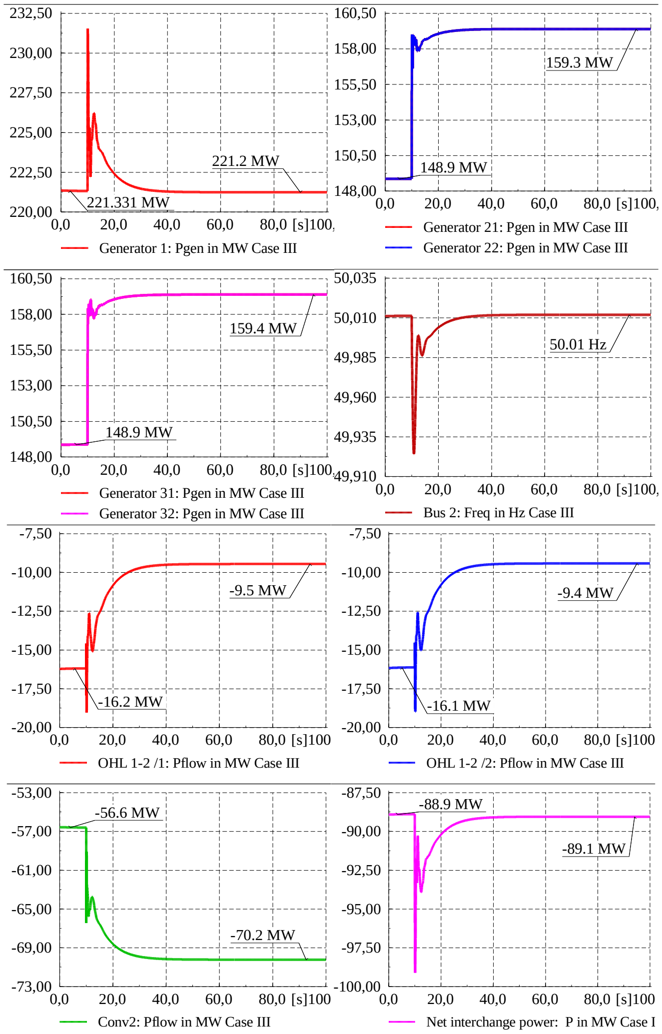

Figure 8. Plots of main electromechanical: *Case III.*

VII. Acknowledgements

This study was partially supported in part by the Chilean National Commission for Scientific and Technological Research (CONICYT) and British Council under the UKIERI, under grant Fondecyt 1130793 and IND/CONT/E/13-14/700, respectively.

VIII. References

[1] F. Gonzalez-Longatt, "Frequency Control and Inertial Response Schemes for the Future Power Networks," in *Large Scale Renewable Power Generation*, J. Hossain and A. Mahmud, Eds., ed: Springer Singapore, 2014, pp. 193-231.

[2] F. Gonzalez-Longatt, "Frequency Control and Inertial Response Schemes for the Future Power Networks," in *Advances in Technologies for Generation, Transmission and Storage, Green Energy and Technology Series*. vol. VIII, J. Hossain and A. Mahmud, Eds., ed Singapur: Springer-Verlag, 2014, p. 363.

[3] F. Gonzalez-Longatt, "TUTORIAL: Frequency Control and Inertia Response Schemes for the Future Power Networks," presented at the IEEE Inernational Energy Conference and Exhibition, ENERGYCON 2012, Florence, Italy, 2012.

[4] F. Gonzalez-Longatt, "Impact of synthetic inertia from wind power on the protection/control schemes of future power systems: Simulation study," in *Developments in Power Systems Protection, 2012. DPSP 2012. 11th International Conference on*, 2012, pp. 1-6.

[5] P. Wall, "Online Prediction of the Post-Disturbance Frequency Behaviour of a Power System," Doctor of Philosophy, School of Electrical and Electronic Engineering, The University of Manchester, Manchester, UK, 2013.

[6] Z. Jiebei, C. D. Booth, G. P. Adam, and A. J. Roscoe, "Inertia emulation control of VSC-HVDC transmission system," in *Advanced Power System Automation and Protection (APAP), 2011 International Conference on*, 2011, pp. 1-6.

[7] Z. Jiebei, C. D. Booth, G. P. Adam, A. J. Roscoe, and C. G. Bright, "Inertia Emulation Control Strategy for VSC-HVDC Transmission Systems," *Power Systems, IEEE Transactions on*, vol. 28, pp. 1277-1287, 2013.

[8] Z. Jiebei, J. M. Guerrero, C. D. Booth, Z. Haotian, and G. P. Adam, "A generic Inertia Emulation Controller for multi-terminal VSC-HVDC systems," in *Renewable Power Generation Conference (RPG 2013), 2nd IET*, 2013, pp. 1-6.

[9] Y. Phulpin, "Communication-Free Inertia and Frequency Control for Wind Generators Connected by an HVDC-Link," *Power Systems, IEEE Transactions on*, vol. 27, pp. 1136-1137, 2012.

[10] G. Fujita, G. Shirai, and R. Yokoyama, "Automatic generation control for DC-link power system," in *Transmission and Distribution Conference and Exhibition 2002: Asia Pacific. IEEE/PES*, 2002, pp. 1584-1588 vol.3.

[11] P. F. de Toledo, P. Jiuping, K. Srivastava, W. WeiGuo, and H. Chao, "Case Study of a Multi-Infeed HVDC System," in *Power System Technology and IEEE Power India Conference, 2008. POWERCON 2008. Joint International Conference on*, 2008, pp. 1-7.

[12] J. Dai, Y. Phulpin, A. Sarlette, and D. Ernst, "Coordinated primary frequency control among non-synchronous systems connected by a multi-terminal high-voltage direct current grid," *Generation, Transmission & Distribution, IET*, vol. 6, pp. 99-108, 2012.

[13] B. Silva, C. L. Moreira, L. Seca, Y. Phulpin, and J. A. Peas Lopes, "Provision of Inertial and Primary Frequency Control Services Using Offshore Multiterminal HVDC Networks," *Sustainable Energy, IEEE Transactions on*, vol. 3, pp. 800-808, 2012.

[14] ENTSO-e. (2009). *P1 – Policy 1: Load-Frequency Control and Performance*. Available: https://www.entsoe.eu/fileadmin/user_upload/_library/publications/entsoe/Operation_Handbook/Policy_1_final.pdf

[15] NGT. (2014). *The Grid Code -ISSUE 5 REVISION 11, 21 August 2014*. Available: http://www2.nationalgrid.com/UK/Industry-information/Electricity-codes/Grid-code/The-Grid-code/

[16] H. Bevrani and T. Hiyama, *Intelligent automatic generation control*. Boca Raton: Taylor & Francis, 2011.

[17] J. Machowski, J. W. Bialek, and J. R. Bumby, *Power system dynamics : stability and control*, 2nd ed. Chichester, U.K.: Wiley, 2008.

[18] H. Shayeghi, H. A. Shayanfar, and A. Jalili, "Load frequency control strategies: A state-of-the-art survey for the researcher," *Energy Conversion and Management*, vol. 50, pp. 344-353, 2// 2009.

[19] I. Ibraheem, P. Kumar, and D. P. Kothari, "Recent philosophies of automatic generation control strategies in power systems," *Power Systems, IEEE Transactions on*, vol. 20, pp. 346-357, 2005.

[20] V. Pavlovsky and A. Steliuk, "Modelling of automatic generation control in power systems," in *PowerFactory Applications for Power System Analysis*. vol. 1, F. M. Gonzalez-Longatt, Luis Rueda, Jose (Eds.), Ed., First Edition ed: Springer, 2014, p. 582.

[21] P. Kundur, N. J. Balu, and M. G. Lauby, *Power system stability and control*. New York: McGraw-Hill, 1994.

[22] F. Milano, *Power system modelling and scripting*. London: Springer, 2010.

[23] F. Gonzalez-Longatt. (2014). *IEEE 14 bus Test: Power system test case archive*. Available: http://fglongatt.org/OLD/Test_Case_IEEE_14.html